AIP | Applied Physics Letters

Experimental observation of leaky modes and plasmons in a hybrid resonance element

R. Magnusson, H. G. Svavarsson, J. Yoon, M. Shokooh-Saremi, and S. H. Song

Citation: Appl. Phys. Lett. **100**, 091106 (2012); doi: 10.1063/1.3690951
View online: http://dx.doi.org/10.1063/1.3690951
View Table of Contents: http://apl.aip.org/resource/1/APPLAB/v100/i9
Published by the American Institute of Physics.

Experimental observation of leaky modes and plasmons in a hybrid resonance element

R. Magnusson,[1,a)] H. G. Svavarsson,[2] J. Yoon,[1] M. Shokooh-Saremi,[3] and S. H. Song[4]
[1]*Department of Electrical Engineering, University of Texas-Arlington, Arlington, Texas 76019, USA*
[2]*School of Science and Engineering, Reykjavik University, Reykjavik, Iceland*
[3]*Department of Electrical Engineering, Ferdowsi University of Mashhad, Mashhad, Iran*
[4]*Department of Physics, Hanyang University, Seoul, Korea*

(Received 6 January 2012; accepted 11 February 2012; published online 29 February 2012)

We provide experimental evidence of a hybrid photonic device supporting simultaneously surface-plasmon polaritons and resonant leaky modes. A fabricated metallo-dielectric structure exhibits a pronounced plasmonic resonance at 799 nm wavelength and a modal resonance at 669 nm in transverse magnetic polarization. In transverse electric polarization, a weak modal resonance appears at 725 nm wavelength. We identify the corresponding modes by computing the attendant internal field distributions. Numerically computed spectra are in good agreement with our measurements. Since traditional modal and plasmonic devices find many uses, their hybrid versions may enable the extension of their applicability. © *2012 American Institute of Physics*. [http://dx.doi.org/10.1063/1.3690951]

There is great interest in the fundamental physical properties of surface plasmon polaritons (SPPs) motivated partly by their applicability in nano-scale photonic devices and sensors. As widely discussed, SPPs exist on metal/dielectric interfaces.[1,2] As the wave vector of a SPP existing on a flat metal/dielectric interface does not match the incident wave vector, an in-plane phase (momentum) matching scheme is employed for its excitation. Often the metal surface itself is periodic to implement the momentum matching. Alternatively, by placing a dielectric or semiconductor grating adjacent to a homogeneous metal film or metal substrate, SPPs can be similarly excited. Müller *et al*. applied shallow photoresist gratings to demonstrate experimentally light absorption on coupling with SPPs on a Au/Ag layer system.[3] Salakhutdinov *et al*. considered a metal surface with a dielectric grating to realize enhanced diffraction efficiency by engaging resonant leaky modes.[4] Seshadri conducted numerical analysis of a planar dielectric film waveguide on a metal substrate and showed absorption spectra associated with guided modes and SPP coupling.[5] Employing microwave radiation with wavelengths near 1 cm illuminating a wax grating on an aluminum-alloy substrate, Hibbins and Sambles studied the coupling of the input waves to SPPs.[6] Yoon *et al*. conducted experimental studies on a dielectric grating on a silver film; their interest was to compare the measured SPP photonic band gaps to the corresponding theoretically computed band structure.[7] Conducting theoretical simulations on a Ag surface coated with a dielectric grating, Li *et al*. calculated absorption spectra and band structure for supported SPPs and waveguide modes.[8]

Analogous with SPP excitation, metal-free nanopatterned films with subwavelength periods can couple incident light to the leaky eigenmodes of an optical waveguide system if the corresponding phase-matching condition is satisfied.[9,10] On excitation of the eigenmode, a guided-mode resonance (GMR) occurs. This class of resonance elements has a substantial application potential as well,[11] perhaps exceeding that of the class of SPP devices.

Whereas the distinct GMR and SPP resonance effects and applications have been intensively studied during the past decades, there has been, by comparison, minimal research on the devices supporting both resonance effects simultaneously, notwithstanding the papers cited.[3–8] It is of interest to characterize in detail the spectral response of hybrid SPP/GMR elements and analyze their mode structure by detailed field computations at each spectral resonance location. This is motivated by applications including integration of SPP-carrying conductors within CMOS chips as well as advanced hybrid GMR/SPP biosensors. Therefore, in this letter, we present computed spectra pertaining to representative hybrid resonance structures and show detailed field distributions that clarify how the SPPs and leaky modes locate in the device. A working photonic SPP/GMR element is verified experimentally by measured reflectance spectra for both transverse magnetic (TM) and transverse electric (TE) polarization states. We find good agreement between numerical and experimental results.

Figure 1(a) illustrates the device structure. The substrate is gold (Au) with a wavelength-dependent complex refractive index.[12] A dielectric grating with period of $\Lambda = 600$ nm, thickness d, and fill factor $F = 0.4$ attaches to the gold substrate as shown. The refractive index of the dielectric is set to 1.60. Figure 1(b) shows the reflection response of this element under normal incidence for thin ($d = 100$ nm) and thick ($d = 900$ nm) gratings for TM polarization. As seen in Fig. 1(b), in the small thickness case, only one reflection dip appears, which corresponds to the excitation of a classic SPP. However, by increasing the thickness to 900 nm, in addition to SPP, GMR features emerge, corresponding to three quasi-guided modes. For TM polarization, Fig. 1(c) displays the distribution of the magnetic field inside the grating and surrounding media when the grating thickness is 100 nm at the SPP resonance wavelength. As shown, only a

a)Author to whom correspondence should be addressed. Electronic mail: magnusson@uta.edu.

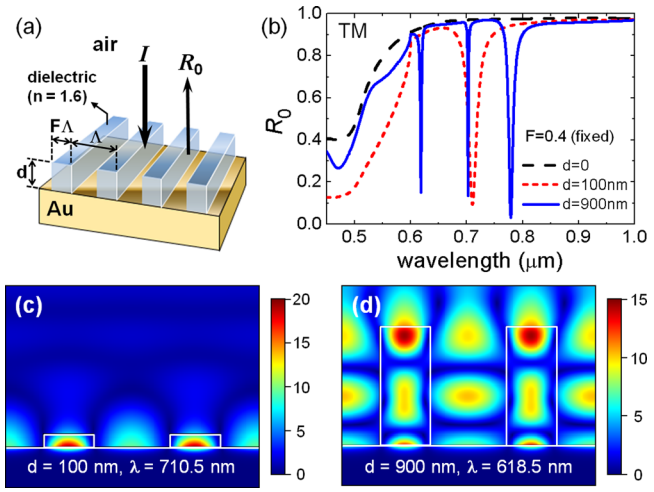

FIG. 1. (Color online) (a) Schematic of the hybrid element that is a dielectric grating placed over a gold substrate. The period of the grating, its thickness, and its fill factor are denoted by Λ, d, and F, respectively. TM (TE) polarized incident light has its magnetic (electric) field vector normal to the plane of incidence. (b) Reflection response of the element versus grating thickness, d, for TM polarization. The SPP resonance is located at 710.5 nm (d = 100 nm), and mixed SPP and leaky-mode resonances are located at 618.5 nm, 702.6 nm, and 778.8 nm (d = 900 nm). The total magnetic field distribution (|**H**|) for (c) the pure SPP excitation at 710.5 nm for d = 100 nm and (d) the mixed SPP and leaky-mode excitation at 618.5 nm for d = 900 nm. In the calculations, the Au substrate is modeled using the frequency-dependent complex refractive index provided by Johnson and Christy in Ref. 12.

SPP standing-wave field is excited and observable with characteristic location on the metal interface. Figure 1(d) shows the magnetic field magnitude for one of the reflection minima at $\lambda = 618.5$ nm when d = 900 nm. Here, SPP-like field concentration at the metal surface as well as leaky modes (TM_2) residing largely in the dielectric are visible. For this case of normal incidence, contra-directional traveling modes are excited, exhibiting attendant standing wave features in the characteristic TM_2 mode shape. For the other two reflection minima at the longer wavelengths, calculations show analogous magnetic field profiles with ~TM_1 (at 703 nm) and ~TM_0 (at 779 nm) modal attributes. Similarly, calculations for TE polarization reveal the existence of ~TE_1- and ~TE_0-type leaky-mode field structures in the same spectral region. This grating is a symmetric structure; therefore, a GMR locates only at one edge of the second stop band.[11] These numerical computations are conducted using rigorous coupled-wave analysis.[13]

To fabricate the device, a sputtering system with a high-purity gold target is used to deposit a gold film on a polished 2 in. Si-wafer substrate at a rate of ~1 nm/s. After deposition, the gold film on the wafer is spin-coated with a positive photoresist (PR) at 500 rpm and cured on a heating plate, adjusted to 110 °C, for 60 s. The PR film is exposed with light from a continuous-wave laser interference system with a wavelength of $\lambda = 266$ nm and intensity of 0.1 mW/cm^2. The period Λ of the resulting resist pattern is given by $\lambda/2 \sin\theta$, where λ is the wavelength and θ is the angle of incidence of the incoming light for the symmetric incidence case.

A scanning electron microscope (SEM) is used to characterize the sample. The thickness of the dielectric (PR) grating is ~560 nm as determined from the SEM cross section in Fig. 2. Its ridge width is found as ~220 nm, which corresponds to a filling factor F ~ 0.37. As seen, the sidewalls are not fully vertical, and thus, a weighted average of the top and bottom widths is taken for the theoretical comparison.

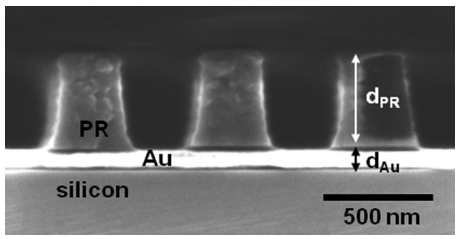

FIG. 2. A cross-sectional SEM micrograph of the fabricated element.

The resonance properties of the devices are explored using reflectance spectroscopy in the wavelength range of $\lambda = 400$–1000 nm. A deuterium-tungsten lamp is used as a light source. Zero-order reflectance (R_0) spectra are measured under normal incidence. Normalized measured reflectance is shown in Fig. 3 for both polarization states. For a comparison, the computed spectra are plotted in the same graphs. The fitting parameters for the spectral calculation are $\Lambda = 653$ nm, $d_{PR} = 560$ nm, $d_{Au} = 80$ nm, n = 1.6, and F = 0.35. The complex and dispersive refractive indices for Au and Si are taken into account. Resonance features of the TM and TE modes are apparent as drops in the R_0 intensity occur on coupling to the lossy metal surface. The total internal field distribution patterns corresponding to the experimental resonance positions are shown in Fig. 4.

A good match between the computed and the experimental data is observed for both TE and TM polarized light. As seen, two resonance minima in the TM spectrum appear. The resonance at the ~799 nm wavelength is related to the excitation of a classic SPP; the other resonance (TM_1) at ~669 nm corresponds to a GMR. In the TE case, the only

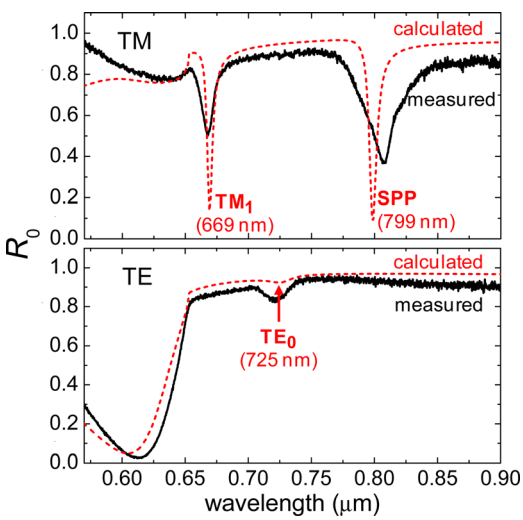

FIG. 3. (Color online) Measured reflectance of the element (solid curve) drawn against the computed reflectance spectra (dashed curve) under normal incidence for TM polarization (top) and TE polarization (bottom). The structural parameters in the calculation are $\Lambda = 653$ nm (consistent with the Rayleigh anomaly at 653 nm in the measured spectra), F = 0.35 (this gives best fit for the TM resonance positions; TE resonance is relatively insensitive to F), and Au thickness = 80 nm (based on the SEM image in Fig. 2).

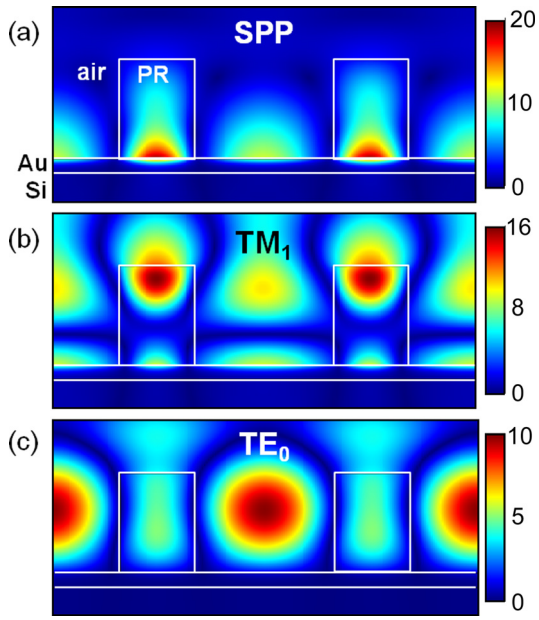

FIG. 4. (Color online) Total magnetic field distributions (|H|) for (a) SPP and (b) TM_1 mode excitations. (c) Total electric field distribution (|E|) for TE_0 mode excitation. The associated resonance responses and locations in the reflection spectra are indicated in Fig. 3.

resonance observed (TE_0) is related to the excitation of leaky modes, since SPP resonances only appear when the polarization of incident light is in the TM state. These observations are further justified by Fig. 4 where the magnetic and electric field distributions at the resonance wavelengths in Fig. 3 are shown. As displayed in Figs. 4(a) and 4(b), the structure supports a surface-plasmon resonance at the longer wavelength (799 nm) and a GMR for TM light at the shorter wavelength (669 nm). In contrast, only a GMR is observed for TE light as shown in Fig. 4(c) without any field concentration at the metal/dielectric interface.

In conclusion, experimental evidence of a photonic device supporting simultaneously SPP and GMR types of resonances has been provided. A fabricated metallo-dielectric structure exhibits a pronounced plasmonic resonance at 799 nm wavelength and a modal resonance at 669 nm in TM polarization. The attendant field distributions defining the resonant modes are verified by theoretical simulations. In TE polarization, a weak modal resonance appears at the 725 nm wavelength. Traditional SPP and GMR devices are of use in many applications; their hybrid versions may enable an extension of their potential as well as provide routes to advanced device embodiments grounded in these fundamental resonance effects.

This research was supported in part by the UT System Texas Nanoelectronics Research Superiority Award funded by the State of Texas Emerging Technology Fund. Additional support was provided by the Texas Instruments Distinguished University Chair in Nanoelectronics endowment.

[1]H. Raether, *Surface Plasmons on Smooth Surfaces and on Gratings* (Springer, Berlin, 1988).
[2]S. A. Maier, *Plasmonics: Fundamentals and Applications* (Springer, New York, 2007).
[3]K. L. Müller, M. Veith, S. Mittler-Neher, and W. Knoll, J. Appl. Phys. **82**, 4172 (1997).
[4]I. F. Salakhutdinov, V. A. Sychugov, and O. Parriaux, Quantum Electron. **28**, 983 (1998).
[5]S. R. Seshadri, J. Opt. Soc. Am. A **16**, 922 (1999).
[6]A. P. Hibbins and J. R. Sambles, Phys. Rev. E **61**, 5900 (2000).
[7]J. Yoon, G. Lee, S. H. Song, C.-H. Oh, and P.-S. Kim, J. Appl. Phys. **94**, 123 (2003).
[8]X. Li, D. Han, F. Wu, C. Xu, X. Liu, and J. Zi, J. Phys. Condens. Matter **20**, 1 (2008).
[9]R. Magnusson and S. S. Wang, Appl. Phys. Lett. **61**, 1022 (1992).
[10]S. S. Wang and R. Magnusson, Appl. Opt. **32**, 2606 (1993).
[11]Y. Ding and R. Magnusson, Opt. Express **12**, 5661 (2004).
[12]P. B. Johnson and R. W. Christy, Phys. Rev. B **6**, 4370 (1972).
[13]T. K. Gaylord and M. G. Moharam, Proc. IEEE **73**, 894 (1985).